

Size effect on toughness property of strain hardening cementitious composite

S.L. Xu, L.J. Hou & X.F. Zhang

Dalian University of Technology, Dalian, P.R. China

ABSTRACT: This paper presents the results of an experimental investigation to determine the size effect on flexural toughness of high performance short fiber reinforced cementitious composite incorporating a low fiber volume fraction of 2% and showing excellent tensile strain hardening capacity in excess of 3%. Evaluation of toughness was made using a pair of new proposed parameters, i.e., flexural strength and energy dissipation per unit volume of plastic hinge region, termed as σ and T_v , respectively. Five groups of strain hardening cementitious composite specimens with constant length of 400mm and width of 100mm but varying thickness of 15mm, 30mm, 50mm, 70mm and 100mm were investigated. Four-point bending tests were carried out under displacement control at the rate of 0.15mm/min. Referring to ASTM C 1609 toughness testing procedure, 100mm thickness specimens were identified as the control and four pairs of additional toughness parameters ($\sigma_{v,1.0}$, $T_{v,1.0}$; $\sigma_{v,1.5}$, $T_{v,1.5}$; $\sigma_{v,2.5}$, $T_{v,2.5}$; $\sigma_{v,3.0}$, $T_{v,3.0}$) were recommended with the consideration of remarkable deflection hardening behavior of such materials prior to the reach of peak load. For other series of specimens' thickness, the deflection governing points at which toughness properties were calculated were determined by multiplying the deflection values of 100mm thickness specimens by a transforming factor defined as a function of specimens' thickness. It was found that two toughness parameters at all seven governing points have nothing to do with specimens' thickness, being no size effect. Further theoretical dimension analysis proves such experimental observations.

1 INSTRUCTION

Utilization of fiber to improve the brittleness property of plain concrete was earliest reported in 1960s (Romualdi & Batson 1963, Mandel 1964). Since then, extensive investigations on toughness improvement of fiber reinforced concretes (FRCs) have been conducted by many researchers. In recent years, significant progresses on FRCs have been obtained. A tension strain hardening cementitious composite reinforced with discrete short fiber, termed as engineered cementitious composite (ECC), was proposed by V.C. Li et al. in 1990s (Li & Leung 1992). In addition to owning high fracture energy of 24KJm^{-2} (Li & Hashida 1993), this material has excellent tension ability of tensile strain up to 2%~6% and perfect crack dispersing capability with maximum crack width of $100\mu\text{m}$ at the ultimate state (Li et al. 2001). Recently, ultra high toughness cementitious composite (UHTCC) (Xu & Li 2008), similar to ECC, has been come true in China through the persisting investigations of several years. UHTCC contains a low fiber volume fraction of 2%, but has a tensile strain up to 3% or higher, along with remarkable flexural toughness and crack controlling capacity highly superior to ordinary FRC (Li 2008).

The toughness property, as an excellent merit of FRC especially the tension strain hardening cementi-

tious composite, is generally evaluated through flexural test. Currently, there are two often-used standard methods to estimate such a performance, for instance, the ASTM C 1018 (ASTM C 1018 1997) and JCI SF-4 (JCI Standard SF-4 1984). The nondimensional value is obtained by ASTM C 1018 method, where the first cracking load and corresponding mid-span deflection are respectively defined as reference value of toughness calculations. However, because the first cracking moment in FRC is rather difficult (Naaman & Reinhardt 1996, Chanvillard 1999), the calculated toughness of FRC especially ones with low fiber fraction is less accurate (Balaguru et al. 1992, Mindness et al. 1994). Unlike the ASTM C 1018, the absolute value is given based on the JCI SF-4 method. It is more effective in the case when to be used to estimate the toughness capacity of FRC with low fiber fraction (Shah et al 1995). Taking into account the drawbacks in the ASTM C 1018, the modified standard method ASTM C 1609 (ASTM C 1609 2005) was proposed in 2005, in which the absolute value, similar to the JCI SF-4 method, is adopted and thus the determination of first cracking point is avoided. ASTM C 1609 is with success used to evaluate the toughness ability of FRC containing small amount of steel fibers and performing post-crack strain-softening (Marijan & Dubravka 2008). Nevertheless, in the case of FRC with high amount of fibers and deflection hardening

property (Marijan & Dubravka 2008), applicability of ASTM C 1609 is not yet clear.

Due to the lack of a uniform standard method used to evaluate the toughness property of tensile strain hardening FRC, some investigators chose the thin plate specimen with 15mm in depth (Tian 2008), while others chose the small beam specimen of 100mm deep (Li 2008) referring to the current toughness test method. The toughness capacity is estimated by ASTM C 1018 or JCI SF-4, and the results obtained are only available to be compared for a specific thickness. But it remains unknown with respect to the toughness performance between the different depths.

The current paper presents four-point flexural experiments of tension strain hardening cementitious composite to investigate the size effect on toughness property. In the evaluation of toughness, two parameters were introduced. One is flexural strength, i.e., σ ; the other proposed is energy absorption per unit volume of plastic hinge region, i.e., T_v . And the further theoretical explanation, with respect to the relation between T_v and thickness is subsequently given.

2 EXPERIMENTAL PROGRAM

2.1 Materials

The matrix of UHTCC consists of cement, fine sand, fly ash and mineral addition. The reinforced fiber was synthetic PVA fiber manufactured by Kuraray Co., Ltd of Japan. The fiber is 12mm long, 0.04mm in diameter, which corresponds to an aspect ratio of 300. The strength of the fiber is 1600 MPa, with an tension elasticity of 42 GPa. The volume fraction of PVA fiber was 2%. A Hobart mixer with the maximum capacity of 12L was used to produce UHTCC. The dry constituents of UHTCC were firstly mixed for about 1-2 minutes. Then, water was slowly added into the mixer. Subsequently, a small dosage of superplasticizer was added in order to obtain a good workability of fresh matrix. Finally, the fiber was slowly added into the mixer by hand. When uniform fiber dispersion was observed, the mixing was completed.

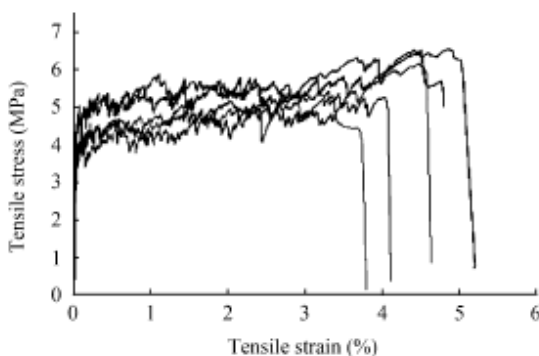


Figure 1. The tensile stress-strain curves of UHTCC obtained by uniaxial tension test.

2.2 Specimen Fabrication and Test Set-up

In this test, all specimens were 400mm long, 100mm wide. The thickness was only a varying parameter. Five groups of specimens, of which the thickness were 15mm, 30mm, 50mm, 70mm and 100mm, respectively, were casted. They were labeled as Sf15, Sf30, Sf50, Sf70 and Sf100, respectively. In each group, three specimens were prepared. At the same time, three compression cubes of 70×70×70mm were also prepared to evaluate the compressive strength of UHTCC. At the age of 24h, the specimens were demoulded and moved into curing room. The temperature and humidity of curing room were kept at 20 ± 3 °C and 90%. After the curing age of 28d, the specimens were moved out from curing room for an air dry of 24h before testing. The compressive strength of UHTCC tested in the experiment was 44MPa. The uniaxial tension test was performed using a rectangle thin plate. The detailed testing procedure can be found in the literature (Li 2008). The measured uniaxial tensile stress-strain curves were shown in Figure 1. It can be seen that UHTCC exhibits tensile strain hardening characteristics.

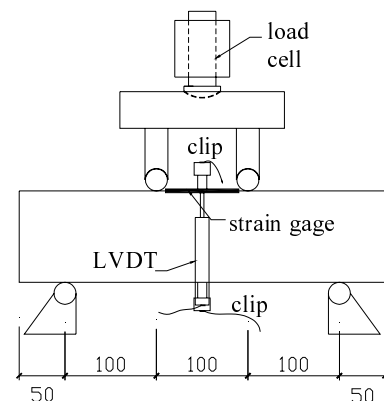


Figure 2. The set-up of four-point bending test.

The four-point bending test was carried out on the 1000kN electric electro-hydraulic servo-controlled test machine. The load was applied in a displacement control loading manner, and the loading rate of 0.15mm/min was chosen. To obtain a high accuracy of load as much as possible, a small load transducer with the maximum measurement of 5t was connected to the loading plate of the testing machine. Two linear variable differential transformers (LVDTs) were fixed at the middle span of specimens to record the deflection of middle span. In addition, a strain gage was stuck on the top to measure the compressive strain on the top of cross section. And two clips equipped on the top and bottom of specimens in pure flexural region, were also used to investigate the evolution of tensile strain and compressive strains at the tension and compression ex-

treme fibers of specimens during loading, respectively. The test set-up was shown in Figure 2.

3 EXPERIMENTAL RESULTS AND TOUGHNESS EVALUATION

3.1 Load-deflection Curve and Nominal Flexural Stress-the Maximum Relative Strain Curve

Figure 3a-e illustrate the recorded load-deflection curves for five typical specimens picked from five depth series. As expected, these plots all show the feature of deflection hardening. For investigated specimens, as the thickness increases, the peak load increases from 1kN for specimen with 15mm in depth to 46kN for that with 100mm in depth, whereas the corresponding deflection decreases from 25mm to 3.6mm. Figure 3f shows the variation of both peak load and deflection as a function of specimens' thickness, together with their respective nonlinear fitting plot. It is found that, as specimens' thickness increases, the deflection exhibits a reduction with the relationship in power of -1 whereas for the peak load the relationship in power of 2 is observed.

Figure 4 shows the plots of nominal flexural stress versus the maximum relative strain for five specimens shown in Figure 3. The nominal flexural stress σ (Sun et al. 2002) and maximum relative strain ε_{t-c} (Park & Pauley 1985) are calculated as follows.

$$\sigma = \frac{F}{bh^2l} \quad (1)$$

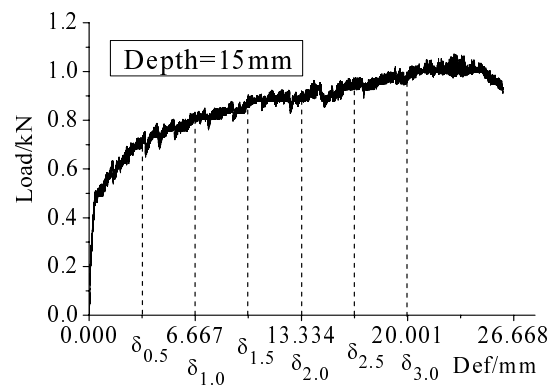
$$\varepsilon_{t-c} = \varepsilon_t - \varepsilon_c = \varphi \cdot h \quad (2)$$

in which, ε_t , ε_c are the tensile or compressive strain at the extreme tension or compression fiber, respectively; b , h are the width and depth of cross section; l is the span length; φ is the curvature of the cross section; ε_{t-c} is the maximum relative strain, defined as the difference between the tensile strain ε_t and the compressive strain ε_c .

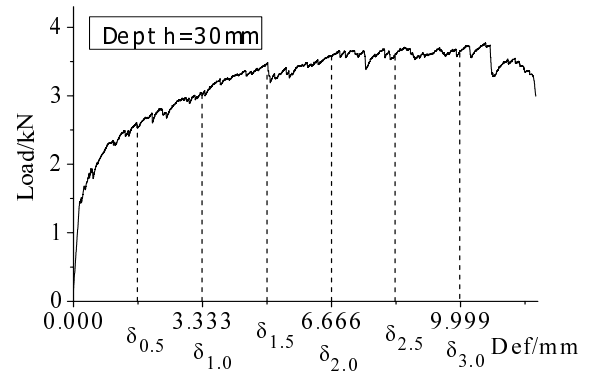
From Figure 4, it is observed that the curves of nominal flexural stress versus the maximum relative strain of five series differ slightly each other. At the ultimate failure, the nominal flexural stress and the corresponding maximum relative strain vary from 12MPa to 14MPa and from 4.3% to 4.8%, respectively. Therefore, it can be concluded that, for strain hardening UHTCC material, no size effect is exhibited on the flexural strength and the maximum relative strain, which is different from plain concrete and traditional fiber reinforced concrete where strain softening behavior occurs after post-cracking.

3.2 Definition of Toughness Evaluation Index

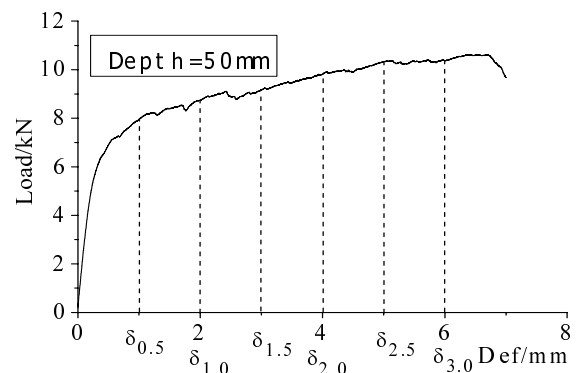
As shown in Figure 3, it is evident that the increasing depth leads to drastic change in terms of load and deflection. Thus, for being convenient to compare with each other, the specimen Sf100, standard one with the dimension of $400 \times 100 \times 100$ mm in span \times width \times depth referring to ASTM C 1609 recommendation standard, is chosen as the control specimen in the following toughness evaluation. The toughness parameters suggested in the method are the load and the area under load-deflection curve at two points where deflections equal to $L/600$ mm (0.5mm) and $L/150$ mm (2.0mm), respectively. Due to the large deflection of Sf100 high to 4mm nearly, apparently, it is not adequate to be used to estimate the toughness of UHTCC with excellent deformation capability. Therefore, the author suggests to take into account more controlling points including $L/600$ mm (0.5mm), $L/300$ mm (1mm), $L/200$ mm (1.5mm),



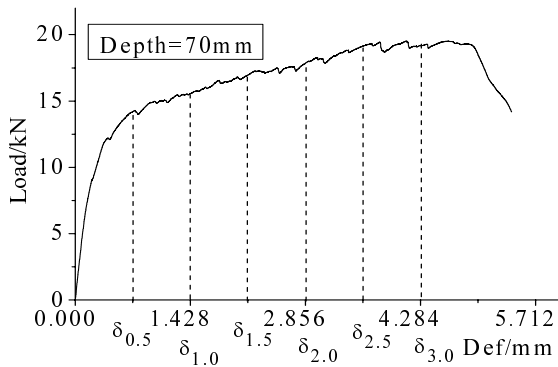
(a) Sf15 series



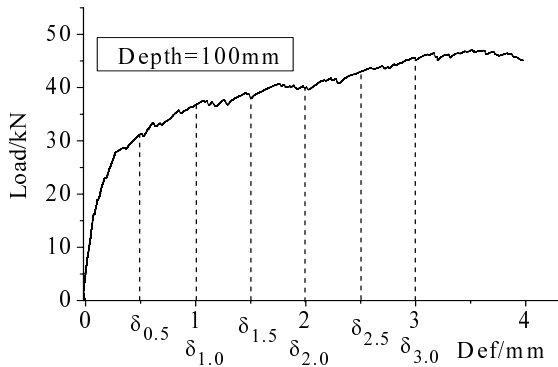
(b) Sf30 series



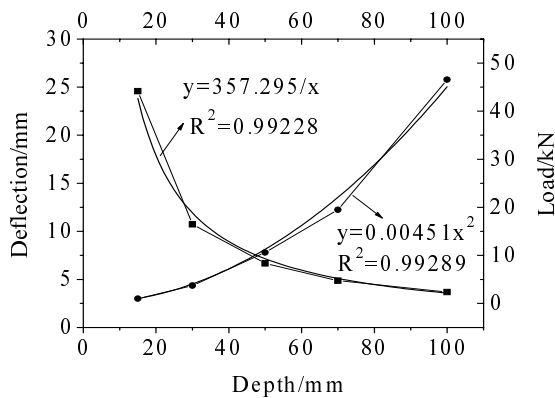
(c) Sf50 series



(d) Sf70 series



(e) Sf100 series



(f) Relations of deflection and load with depth and the fitting curve

Figure 3. Load-deflection curves and determination of transforming deflection points of specimens with different depths.

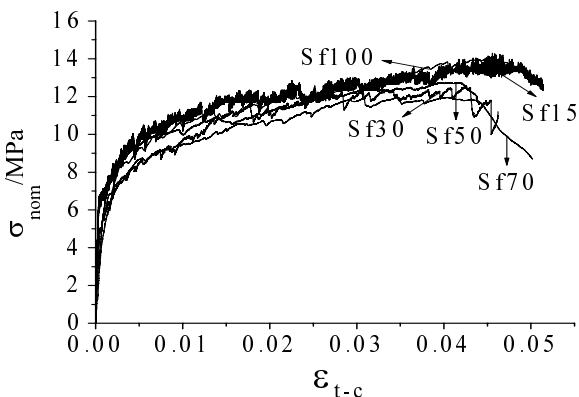


Figure 4. The plots of nominal stress versus the relative strain of five specimens.

L/150mm (2mm), L/120mm (2.5mm), L/100mm (3mm) and the peak load point to evaluate the toughness during the whole deflection hardening stage completely.

From Figure 3, it is found that the deflection at the ultimate failure differs greatly for various depth specimens. The maximum deflection of 25mm occurs in 15mm thickness specimen whereas the minimum deflection of 3.6mm occurs in specimen with 100mm thickness. Obviously, the same deflection controlling points as reference specimen of 100mm deep, as above stated, are not rational to be used to investigate the size effect on toughness of UHTCC by other thinner specimens with a larger deflection.

Based on the inversely proportional relationship between deflection and thickness shown in Figure 3 f, herein, the equivalent deflection points are determined as new controlling points for various series at which the deflection is approximated to the value calculated based on Equation 3, namely $\delta_{0.5}$, $\delta_{1.0}$, $\delta_{1.5}$, $\delta_{2.0}$, $\delta_{2.5}$, $\delta_{3.0}$, respectively.

$$\delta = \delta_{sd} \times 100 / h \quad (3)$$

where δ_{sd} is the deflection of reference specimen Sf100 at controlling point; h is the depth of specimen. Herein, we take two depths as demonstrative examples to further clarify the definition of the equivalent deflection points. For example, in the case of Sf50 with depth of 50mm, the factor $100/h$ in Equation 3 equals 2, and thereby the deflection at the equivalent deflection points corresponding to $\delta_{0.5}$, $\delta_{1.0}$, $\delta_{1.5}$, $\delta_{2.0}$, $\delta_{2.5}$ and $\delta_{3.0}$ are 1mm, 2mm, 3mm, 4mm, 5mm and 6mm, respectively. While, in the case of Sf15 having the depth of only 15mm, the factor $100/h$ in Equation 3 becomes 6.67 and the deflection at the equivalent deflection points are 3.33mm, 6.67mm, 10.00mm, 13.33mm, 16.67mm and 20.00mm, respectively. The equivalent deflections of each depth series at six equivalent deflection points are shown in Figure 3a-e in detail. It should be noted that in addition to the equivalent controlling points, another controlling point δ_{peak} is defined as the tested deflection corresponding to the peak load of various depth series.

For members made of UHTCC, when subjected to four point flexural loading, a great number of fine cracks at a very narrow spacing can be usually observed in the pure bending zone. As the results, in the comparison with the strain softening materials such as plain concrete, it is more rational for strain-hardening material that the span length of pure bending zone is assumed to be the length of plastic hinge zone where the energy consumption during loading will mainly occurs. This had been demonstrated by the reference (Soranakom & Mobasher 2007). In their study, the pure bending region was assumed to be plastic hinge zone without consideration of additional equivalent

plastic hinge zone in shear-span zone. The so calculated deflection at mid-span was found to well agree with the tested results. With these points, a new parameter, which is defined as the energy dissipation per unit volume of plastic hinge region T_v as expressed in Equation 4, is proposed to evaluate the size effect on toughness performance of such materials.

$$T_v = T(\delta) / V_{p-h} \quad (4)$$

where T is the area under the load-deflection curve at equivalent deflection points; V_{p-h} is the volume of plastic hinge region in cases of different series. And the index T_v is termed as $T_{v,0.5}$, $T_{v,1.0}$, $T_{v,1.5}$, $T_{v,2.0}$, $T_{v,2.5}$, $T_{v,3.0}$, and $T_{v,peak}$ at different equivalent controlling points and peak point, respectively.

In addition, similar to the estimation of size effect on flexural property, it is the nominal flexural strength σ rather than the load capacity that seems to be a good parameter estimating the size effect on toughness, named to be $\sigma_{v,0.5}$, $\sigma_{v,1.0}$, $\sigma_{v,1.5}$, $\sigma_{v,2.0}$, $\sigma_{v,2.5}$, $\sigma_{v,3.0}$, and $\sigma_{v,peak}$ for $\delta_{0.5}$, $\delta_{1.0}$, $\delta_{1.5}$, $\delta_{2.0}$, $\delta_{2.5}$, $\delta_{3.0}$, δ_{peak} , respectively.

In summary, after the determination of equivalent governing points in the case of each depth, the proposed two toughness indexes, i.e., σ and T_v , are calculated based on Equation 3 and Equation 4, respectively. Subsequently, the size effect on toughness property can be evaluated by the values of σ and T_v , substituted for the load P and area T toughness indexes.

3.3 Toughness Evaluation

The new toughness index σ and T_v of various series are calculated by applying the Equations 3 and 4. Figure 5 shows the nominal strength toughness index σ at equivalent controlling points in cases of various types. It is revealed that the flexural stress gradually ascends from 8.3MPa to 13.8MPa with the increase in deflection as a whole, whereas the bending strength at the same point is almost comparable each other. The ratio of σ for each depth to the average value of σ at the same deflection point is fairly close to unit 1, with maximum error only being 0.12 as shown in the Figure 6.

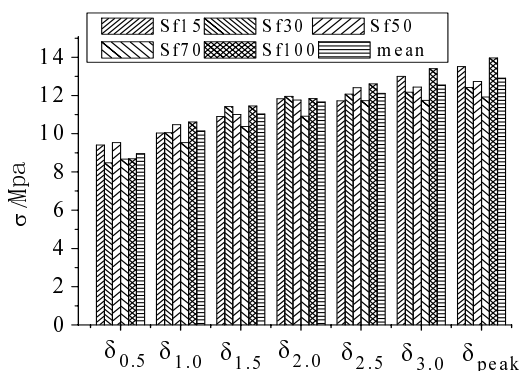


Figure 5. Nominal flexural stress at converting deflection points.

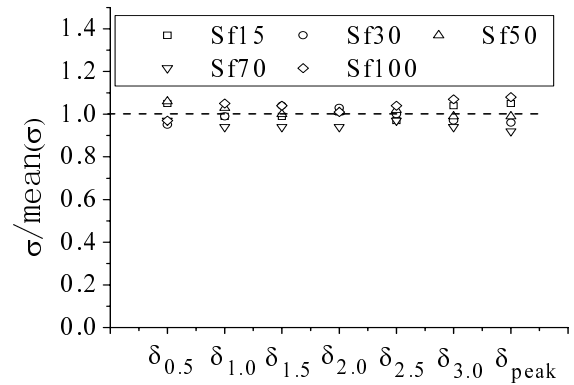


Figure 6. Dimensionless flexural stress at equivalent deflection points.

The toughness index T_v of different depths specimens at seven transforming deflection points was calculated according to the proposed approach in this paper and was shown in Figure 7a-g respectively. In Figure 7, the area toughness index T calculated based on ASTM C 1609 standard are plotted, too. It should be noted that the T_v of the depth of 0mm represents the mean of all T_v values; the narrower columns represent the proposed index T_v ; the wider columns represent the conventional area index T under load-deflection curve of different categories at the transforming points. It is found that the ratios of the area index T of Sf100 to that of other four series ranged from 1.5 to 6 approximately. Apparently, the area index T at the same point changes greatly between different series, showing that the larger thickness the higher T . The possible reason for so great difference is mainly due to the different volume of plastic hinge zone. Therefore, it seems not rational for UHTCC to estimate the toughness of specimens with different depths. In contrast, an interesting finding is noted for the energy absorption per unit volume of plastic hinge region T_v . It is seen from Figure 7 that T_v of different depth specimens remains almost a constant at the same equivalent deflection point.

Figure 8 plots the ratio of T_v of each depth to the averaged T_v of all specimens at each deflection controlling point. It is noticed that the maximum error is almost 0.12 expect for that of 0.25 at the point $\delta_{0.5}$ and δ_{peak} , probably due to the larger influence of stiffness of section in small deformation and the peak deflection that is not conform to the transforming Equation 2, respectively.

In summary, σ and T_v show no size effect of depth and can be considered as the intrinsic properties of UHTCC. And, such parameters can be taken to be toughness indexes analogous to the conventional load P and the area T indexes.

In order to further explain the above conclusion, the theoretical dimension analysis is conducted in the following section. It is noted that the span length l and the width w remain constant in this study. Firstly, based on the Equation 1, the load can be expressed as follows.

$$F = \frac{\sigma b h^2}{l} = F(h^2) \quad (5)$$

And, the mid-span deflection can be calculated by the Equation 6 based on the moment-area method.

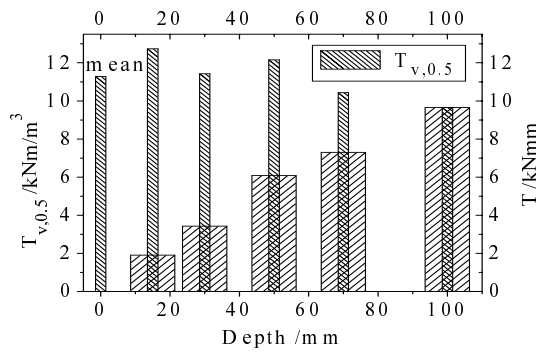
$$\delta = \int_0^{l/2} x \varphi(x) dx \quad (6)$$

where x is the distance between the support and a cross section in mid span; $\varphi(x)$ is the curvature of cross section at x location.

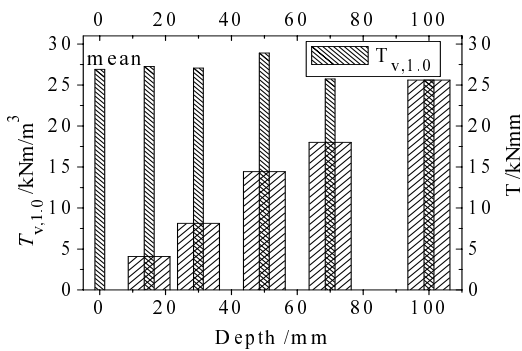
Then, substituting Equation 2 into Equation 6, Equation.7 can be obtained,

$$\delta = \int_0^{l/2} x \cdot \varepsilon_{t-c}(x) \cdot h^{-1} \cdot dx \quad (7)$$

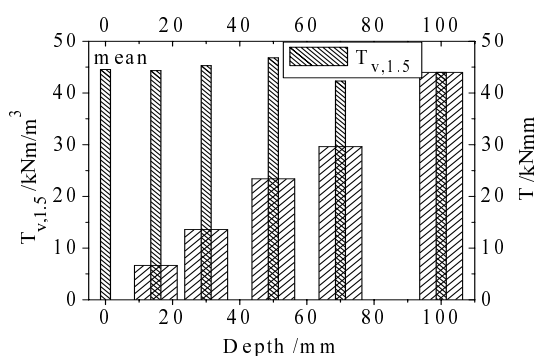
According to ASTM C 1609, area toughness index T can be calculated by the Equation 8. Furthermore, inserting the Equation 5 and Equation 7 into Equation 8, area toughness index T can be recast in the form of Equation 9.



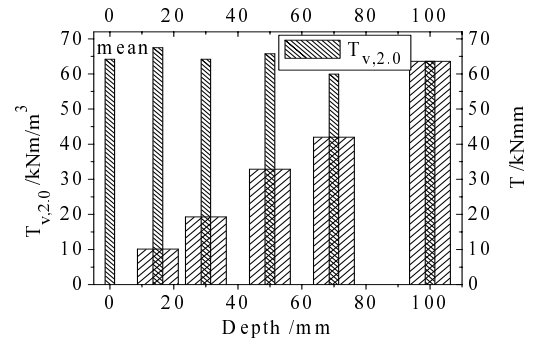
a. Equivalent deflection $\delta_{0.5}$



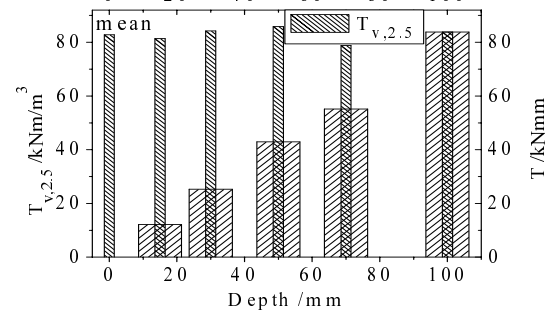
b. Equivalent deflection $\delta_{1.0}$



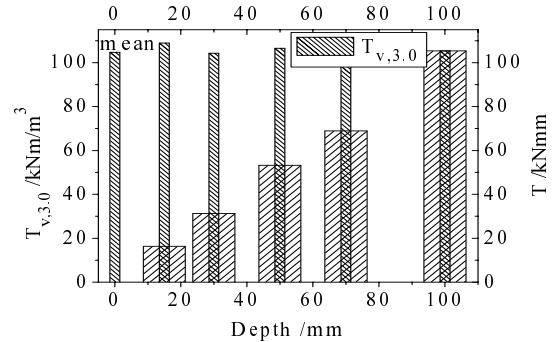
c. Equivalent deflection $\delta_{1.5}$



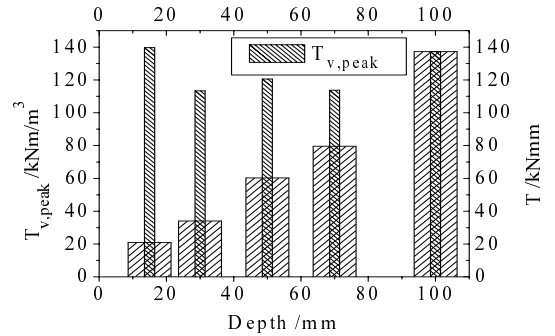
d. Equivalent deflection $\delta_{2.0}$



e. Equivalent deflection $\delta_{2.5}$



f. Equivalent deflection $\delta_{3.0}$



g. Equivalent deflection δ_{peak}

Figure 7. The change of T_v as the depth increases.

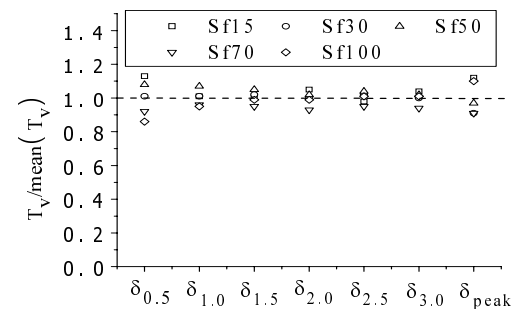


Figure 8. The dimensionless T_v of various specimens at transforming deflection points.

$$T = \int_0^{\delta} F \cdot d\delta \quad (8)$$

$$T = \frac{bh}{l} \cdot \int_0^{l/2} \sigma(x) \varepsilon_{t-c}(x) x dx \quad (9)$$

According to definition for the proposed index T_v , it can be calculated by dividing T by the volume of pure bending region V_{p-h} , as shown in first equality in Equation 4. Then, substituting Equation 9 into Equation 4, Equation 10 can be got.

$$\begin{aligned} T_v &= \frac{T}{V_{p-b}} = 3(bhl)^{-1} \cdot \int_0^{l/2} dT \\ &= 3l^{-2} \cdot \int_0^{l/2} \sigma(x) \varepsilon_{t-c}(x) x dx \end{aligned} \quad (10)$$

In Equation 10, stress $\sigma(x)$ and relative strain $\varepsilon_{t-c}(x)$ are independent on the depth, as shown in Figure 4. Therefore, T_v keeps a constant, identical to tested results.

4 CONCLUSIONS

The four point bending experiments are performed on five depth specimens made of tension strain hardening material to investigate the effect of thickness on toughness capacity. Taking into account that the energy is dissipated in a volume element rather than several plane elements, and the large influence of depth on deflection and load, the two parameter indexes, the flexural strength σ and energy dissipation per unit volume of plastic hinge region T_v at equivalent deflection points, are proposed. Furthermore, more deflection controlling points are considered during the entire deflection hardening stage, in addition to two controlling points given in ASTM C 1609 toughness test standard method. The following conclusions can be drawn from the experiment results and theoretical analysis:

- (1) As depth of specimen increases, the maximum relative strain and nominal strength are almost the same each other.
- (2) The toughness indexes calculated based on the proposed procedure in this paper are almost comparable for various depths at the same equivalent controlling point, while the conventional area index calculated based on ASTM C 1609 standard shows a great difference. Further theoretical dimension analysis accounts for this interesting phenomenon.
- (3) As to UHTCC with tension strain hardening capacity, the proposed two parameters seem to be the intrinsic material properties, that is, without size effect.

REFERENCE

- ASTM C 1018 1997. Standard test method for flexural toughness and first-crack strength of fiber-reinforced concrete (using beam with third-point loading). ASTM International, West Conshohocken.
- ASTM C 1609 2005. Standard test method for flexural performance of fiber-reinforced concrete (using beam with third-point loading). ASTM International, West Conshohocken.
- Balaguru, P., Narahari, R. & Patel, M. 1992. Flexural toughness of steel fiber reinforced concrete. *ACI Materials Journal* 89(6): 541-546.
- Chanvillard, G. 1999. Characterisation of fiber reinforced concrete's performance after a flexural test-part I: on subjectivity of toughness indices. *Materials and Structures* 32: 601-605.
- JCI SF-4, 1984. Method of tests for flexural strength and flexural toughness of fiber-reinforced concrete. Japan Concrete Institute Standards for Test Methods of Fiber Reinforced Concrete. Tokyo.
- Li, H.D. 2008. Experiment research on ultra toughness cementitious composites. PhD thesis. Dalian university of technology.
- Li, V.C. & Leung, C.K.Y. 1992. Theory of Steady State and Multiple Cracking of Random Discontinuous Fiber Reinforced Brittle Matrix Composites. *ASCE Journal of Engineering Mechanics* 118 (11): 2246-2264.
- Li, V.C. & Hashida, T. 1993. Engineering Ductile Fracture In Brittle Matrix Composites. *Journal of Materials Science Letters* 12(12): 898-901.
- Li, V.C., Wang, S. & Wu, C. 2001. Tensile strain-hardening behavior of PVA-ECC. *ACI Materials Journal* 98(6): 483-492.
- Mandel, J.A. 1964. Tensile strength of concrete short affected by uniformly distributed closely spaced short lengths of wire reinforced. *ACI J. Proc.* 61(6): 657-671.
- Marijan, S. & Dubravka, B. 2008. Toughness testing of ultra high performance fiber reinforced concrete. *Materials and Structures* Doi: 10.1617/s 11527-008-9441-3.
- Mindness, S., Chen, L. & Morgan, D. R. 1994. Determination of the first-crack strength and flexural toughness of steel fiber reinforced concrete. *Advanced Cement Based Materials* 1: 201-208.
- Naaman, A.E. & Reinhardt, H.W. 1996. High performance fiber reinforced cement composites 2 (UHPFRCC 2). RILEM Proceedings 31, E&FN Spon.,
- Park, R. & Pauley, T. 1975. *Reinforced concrete structure*. New York: John Wiley & Sons.
- Romualdi, J.P. & Batson, G.B. 1963. Mechanics of crack arrest in concrete. *ASCE Proc.* 89 EM3: 147-168.
- Shah, S.P. et al. 1995. Toughness characterization and toughening mechanisms. In: Naaman AE, Reinhardt HW(eds), Proceedings of the second international RILEM workshop. E & FN Spon, Ann Arbor, USA, 193-228.
- Soranakom, C. & Mobasher, B. 2007. Closed-form solutions for flexural response of fiber reinforced concrete beams. *ASCE Journal of Engineering Mechanics* 133(8): 933-941.
- Sun, X.F., Fang, X.S. & Guan L.T. 2002. *Mechanics of Material*. Beijing: Higher education press.
- Tian, Y.H. 2008. Experimental Research on Self-compacting Ultra High Toughness Cementitious Composite. Masteral thesis. Dalian University of Technology.
- Xu, S.L. & Li, H.D. 2008. A review on the development of research and application of Ultra High Toughness Cementitious Composites, *China Civil Engineering Journal* 41(6): 45-60.